Journal of Colloid and Interface Science 457 (2015) 307–318

Contents lists available at ScienceDirect

Journal of Colloid and Interface Science

journal homepage: www.elsevier.com/locate/jcis

Sulfonated methyl esters of fatty acids in aqueous solutions: Interfacial and micellar properties

Krassimir D. Danov [a], Rumyana D. Stanimirova [a], Peter A. Kralchevsky [a,*], Elka S. Basheva [a], Veronika I. Ivanova [a], Jordan T. Petkov [b]

[a] Department of Chemical & Pharmaceutical Engineering, Faculty of Chemistry & Pharmacy, Sofia University, 1164 Sofia, Bulgaria
[b] KL-Kepong Oleomas SDN BHD, Menara KLK, Jalan PJU 7/6, Mutiara Damansara, 47810 Petaling Jaya, Selangor Dalur Ehsan, Malaysia

GRAPHICAL ABSTRACT

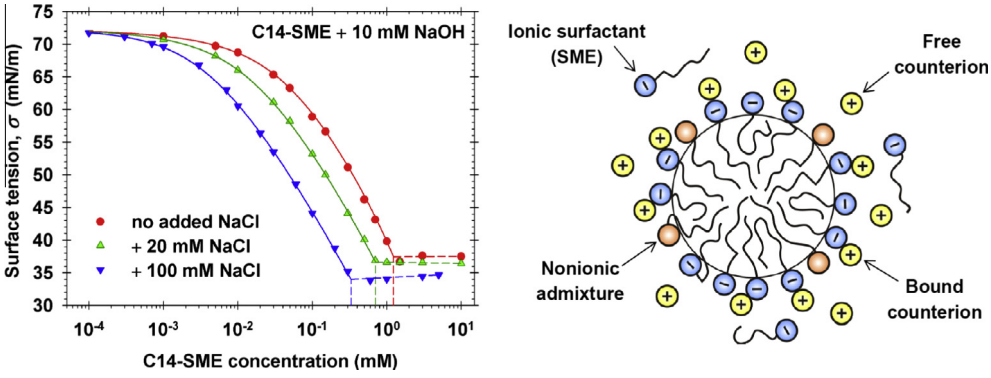

ARTICLE INFO

Article history:
Received 19 May 2015
Revised 9 July 2015
Accepted 9 July 2015
Available online 10 July 2015

Keywords:
Sulfonated methyl esters
Surface tension
Critical micelle concentration
Degree of counterion binding
Micelle surface electric potential

ABSTRACT

The interest to sulfonated methyl esters of fatty acids (SME) has been growing during the last decade, because these surfactants are considered as an environmentally friendly and renewable alternative of the linear alkyl-benzene sulfonates (LAS). Here, we present a quantitative study on the properties of aqueous SME solutions, and especially on their surface tension isotherms, critical micelle concentration (CMC) and its dependence on the concentration of added NaCl. It is demonstrated that the CMC of an ionic surfactant determined by electrical conductivity is insensitive to the presence of a small nonionic admixture, so that the CMC values determined by conductivity represent the CMC of the pure surfactant. Using SME as an example, we have demonstrated the application of a new and powerful method for determining the physicochemical parameters of the pure ionic surfactant by theoretical data analysis ("computer purification") if the used surfactant sample contains nonionic admixtures, which are present as a rule. This method involves fits of the experimental data for surface tension and conductivity by a physicochemical model based on a system of mass-balance, chemical-equilibrium and electric-double-layer equations, which allows us to determine the adsorption and micellization parameters of C12-, C14-, C16- and C18-SME, as well the fraction of nonionic admixtures (if any). Having determined these parameters, we can further predict the interfacial and micellization properties of the surfactant solutions, such as surface tension, adsorption, degree of counterion binding, and surface electric potential at every surfactant, salt and co-surfactant concentrations.

* Corresponding author.
E-mail address: pk@lcpe.uni-sofia.bg (P.A. Kralchevsky).

http://dx.doi.org/10.1016/j.jcis.2015.07.020
0021-9797/

1. Introduction

The sulfonated methyl esters (SME), or α-sulfo fatty acid methyl esters, sodium salts (Fig. 1), represent a relatively new class of biodegradable surfactants [1–4], which are considered as an environmentally friendly alternative of the linear alkyl-benzene sulfonates (LAS) [5]. The production of SME has been growing during the last ten years and currently it stands at more than ten percent of the LAS production. In general, sodium methyl ester sulfonates with random positioning of the SO_3 group in the alkyl chain, known as Φ-MES, have been synthesized [6–11]. Our study is focused on the α-sulfo fatty acid methyl esters (Fig. 1). For brevity, the notation C*n*-SME will be used, where *n* stands for the number of carbon atoms in the fatty-acid chain (n = 12, 14, 16, 18). SMEs are mainly used in cleaning formulations, such as phosphate-free detergent powders [12,13], but they have found applications even in the nanoparticle production [14].

Despite the wide usage of SMEs, their physicochemical characteristics, such as surface tension isotherms, and critical micelle concentration (CMC), published in the literature often differ, sometimes up to order of magnitude in the CMC values [3,14–21]. The lack of clarity on the physicochemical properties of SME has been one of the limitations for increasing the scope of their applications. Our goal here is to address this issue by investigating the surface tension and adsorption properties; critical micellization concentration; ionization degree of micelles and flat adsorption layers, and the effect of added salt.

The most probable reason for the scattering of the literature data for SME solutions is the presence of nonionic admixtures in the used SME samples, which can be different in different batches. This admixture, most probably unsulfonated methyl ester of the respective fatty acid (C*n*-ME), is incorporated in the micelles of the main surfactant and its separation is a difficult experimental task.

Here, we are using the circumstance that it is possible to determine the adsorption and micellar parameters of the ionic surfactant and of the nonionic admixture by computer analysis of experimental data [22,23], without experimental separation of the two species. The experimental data should include (i) surface tension isotherms measured at different NaCl concentrations and (ii) the dependence of the CMC on the concentration of added NaCl. Indeed, the addition of NaCl strongly affects the electro-chemical potential of the ionic surfactant at the solution surface and in the micelles, without essentially influencing the chemical potential of the nonionic surface-active substance. This fact allows one to separate the effects of the ionic and nonionic components and to determine their adsorption and micellization constants by using a quantitative physicochemical model based on chemical-equilibrium and mass-balance equations. Having determined these constants, one can further calculate the surface tension isotherms of the *pure* ionic surfactant and the dependences of its interfacial and micellar properties on the surfactant and salt concentrations.

The paper is organized as follows: Section 2 describes the used materials and experimental methods. Section 3 presents the experimental results from the conductivity and surface-tension measurements. Section 4 describes the theoretical *adsorption* model, its application to determine the adsorption parameters of C*n*-SME and the amount of the nonionic admixture, as well as the model's predictions about the properties of the adsorption layers. Likewise, Section 5 describes the theoretical *micellization* model and its applications. We hope that the obtained results would solve the problem about the controversial literature values for the properties of SME solutions. Moreover, the developed methodology, called for brevity "computer purification", is applicable not only to SMEs, but also to any other ionic surfactant that contains a nonionic admixture.

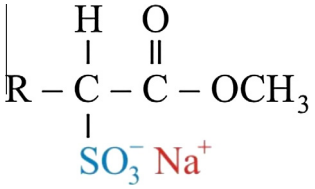

Fig. 1. Structural formula of sulfonated methyl ester (SME); R stands for the alkyl chain.

2. Materials and methods

The used surfactants, produced by the Malaysian Palm Oil Board (MPOB) and KLK OLEO, were sulfonated methyl esters (SME) of different fatty acids: lauric, myristic and palmitic (C12, C14 and C16). In particular, C12-SME, of molecular weight M_w = 316 g/mol, was received as a paste. C14-SME, M_w = 344 g/mol, was received as a dry powder. C16-SME, M_w = 372 g/mol, was supplied as a dry dispersion composed of small flakes. These samples were used in our experiments without any additional purification. The structural formula of the sulfonated methyl esters is shown in Fig. 1.

The used SME samples have been characterized by liquid chromatography–mass spectrometry (LC/MS) analysis. The purity of the used C12-, C14- and C16-SME is, respectively, 97.4%, 97.9% and 96.0%. The admixtures represent small amounts of C*n*-SME with the neighboring even values of *n*. The traces of unsulfonated methyl esters (C*n*-ME) in the used samples are inaccessible to the conventional analytical methods, but they can be registered and quantified by a combination of surface tension and conductivity measurements, as demonstrated below. Karl Fischer analysis has been also carried out to determine the amounts of water in the used SME samples and to work with the correct surfactant concentrations.

Sodium chloride, NaCl (Sigma, Germany, Cat. No 31434), and sodium hydroxide, NaOH (Sigma, Germany, Cat. No 06203), were used as additives. In comparative experiments, sodium dodecyl sulfate (SDS), product of Acros Organics, Pittsburgh, PA, was used.

The aqueous solutions were prepared with deionized water purified by Elix 3 water purification system (Millipore). All experiments were carried out at a temperature of 25 °C.

The equilibrium surface tension, σ, was measured by the Du Noüy ring method using tensiometer K100 (Krüss GmbH, Germany) equipped with a platinum–iridium ring. (Such a ring is optimally wettable because of the very high surface free energy of these two metals.) Before each measurement, the ring was first rinsed with ethanol and then abundantly rinsed with deionized water, followed by heating in a flame to remove any residual organic contaminants. The duration of each measurement was at least 30 min for the higher concentrations and ionic strengths, and 60 min for the lower concentrations.

We carried out measurements of the *electrical conductivity*, κ, of SME solutions with Hanna EC 215 conductivity meter. Before the measurements, the apparatus was calibrated with a standard 10 mM KCl solution. The *pH measurements* were carried out with Hanna pH 211 microprocessor pH-meter.

3. Results on conductivity and surface tension

3.1. CMC determined by conductivity is insensitive to the presence of nonionic admixture

Very often, commercially available ionic surfactants contain a small amount of nonionic surface-active admixture. The

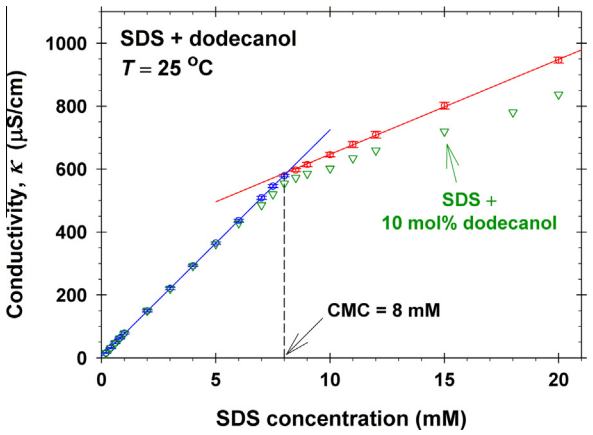

Fig. 2. Conductivity κ vs. SDS concentration. The experimental points obtained with 0, 0.5, 1, 2, 3, 4, 5 and 6 mol% added dodecanol coincide – they are shown by circles with error bars. The kink in the experimental curve (the CMC) is at 8 mM SDS. Difference is observed for 10 mol% added dodecanol (the triangle symbols).

experiment shows that the critical micellization concentration (CMC) of the ionic surfactant determined by *electrical conductivity* measurements does not depend on the presence of such admixture. Hence, the CMC of the pure ionic surfactant can be determined by conductivity measurements, even if the used surfactant sample contains nonionic admixtures. Here, this is demonstrated for SDS with an admixture from dodecanol (Fig. 2). SDS was chosen, because the CMC of pure SDS, 8 mM, is well known [24], unlike the CMCs of the SMEs (see above). Next, conductivity measurements were applied to determine the CMC of C12-, C14- and C16-SME samples, which might also contain nonionic admixtures.

Fig. 2 shows the conductivity κ of SDS solutions with added dodecanol. (The latter plays the role of a nonionic admixture in SDS.) The data indicate that up to 6 mol% (relative to SDS), the dodecanol does not affect the measured conductivity (see also Appendix A). The kink in the conductivity curve corresponds to 8 mM SDS, which is the known literature value of the CMC for pure SDS [24].

It should be expected that at a sufficiently high concentration the effect of dodecanol will show up. Indeed, at 10 mol% added dodecanol, some deviations of the measured conductivity from the respective curve for pure SDS are observed (Fig. 2).

Unlike the conductivity, κ, the equilibrium surface tension, σ, of ionic surfactant solutions is sensitive even to the presence of traces of nonionic admixtures. For example, 0.2 mol% dodecanol (relative to SDS) decreases the surface tension of SDS with about 15 mN/m at concentrations below the CMC; see Fig. 3 in Ref. [22]. The lowering of σ of SDS solutions at concentrations above the CMC can also be considerable; see Fig. A3 in Appendix A. The difference between the values of CMC determined by conductivity and surface tension measurements can be utilized to quantify the amount of nonionic admixture in the ionic surfactant (see below).

3.2. CMC of SME determined by conductivity measurements

The raw data for the pH and conductivity κ of SME solutions are shown in Fig. A1 in Appendix A. Because the pH varies in the range between 4 and 6.5, the measured values of κ are influenced by a contribution from the H^+ ions. To determine the contribution of SME to conductivity, κ_{SME}, the experimental data for κ were processed by using the following equations:

$$\kappa = (\kappa_0 + \lambda^0_H c_H + \lambda^0_{OH} c_{OH} + \kappa_{SME}) f(I) \quad (1)$$

$$f(I) = 1 - 0.7I^{1/2} + 0.74I \quad (2)$$

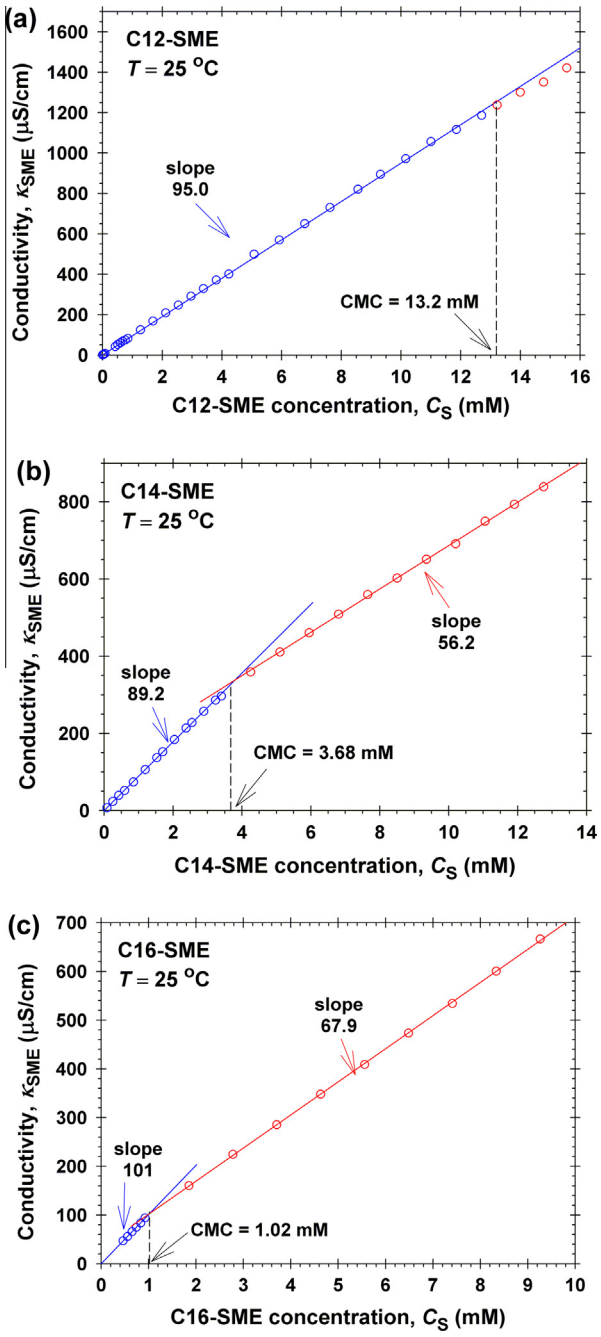

Fig. 3. Conductivity of aqueous C*n*-SME solutions, κ_{SME}, vs. the SME concentration. (a) C12-SME; (b) C14-SME; (c) C16-SME.

Here, c_H and c_{OH} are the concentrations of H^+ and OH^- ions determined from the measured pH and $\lambda^0_H = 349.8$ S cm^2 mol^{-1} and $\lambda^0_{OH} = 199.2$ S cm^2 mol^{-1} are the molar conductances of these ions at infinite dilution [25]; I is the solution's ionic strength; $f(I)$ in Eq. (2) is a semi-empirical expression for the Kohlrausch correction at temperature $T = 25$ °C [25,26]; κ_0 accounts for the background concentration of other ions present in the water and is determined as an adjustable parameter from the data fit with Eqs. (1) and (2).

Fig. 3a–c shows the determined κ_{SME} vs. the SME concentration, C_S, for C12-, C14- and C16-SME. The kinks in the experimental curves correspond to the CMC values, which are given in the figures.

From the Kohlrausch law, we have $\lambda^0_{Na} + \lambda^0_{SME} = \kappa_{SME}/C_S$. The limiting molar conductance of the Na^+ ions is $\lambda^0_{Na} = 50.1$ S cm^2 mol^{-1}

and of the surfactant molecule it is $\lambda^0_{SME} \approx 25$ S cm^2 mol^{-1}; see e.g. Ref. [27]. However, the slopes of the conductivity of SME solutions in Fig. 3a–c (below the CMC) are considerably greater than $\lambda_{SME} \approx 75$ S cm^2 mol^{-1}. These differences indicate the presence of admixture of an inorganic electrolyte in the SME samples. Assuming that the admixture is of NaCl with $\lambda_{NaCl} = 126.5$ S cm^2 mol^{-1}, we estimate that the C12-, C14- and C16-SME samples contain, respectively, 16, 14, and 24 mol% NaCl relative to the surfactant. (A numerically close result for the Na^+ admixture is obtained assuming that the additional electrolyte is Na_2SO_4, because the molar conductance of $1/2Na_2SO_4$ is 130 S cm^2 mol^{-1}, which is close to $\lambda_{NaCl} = 126.5$ S cm^2 mol^{-1} for NaCl; see e.g. Refs. [25,26].) The CMC values in Fig. 3 are affected by the Na^+ counterions due to the admixture of salt. The (slightly higher) CMC's of the pure C*n*-SME, determined by "computer purification", are given in Section 5.3.

3.3. Surface tension isotherms of SME solutions

To suppress the effect of minor fatty-acid admixtures in the used SME samples, which lower the solution's pH (see Appendix A), we measured the surface tension, σ, of SME solutions with added 10 mM NaOH. To investigate the effect of electrolyte on the surface tension of SME solutions, surface tension isotherms were obtained at 0, 20 and 100 mM of added NaCl. The experimental results for C14- and C16-SME are shown in Fig. 4, where the solid lines are the best fits by the van der Waals adsorption model (see Section 4.1).

As seen in Fig. 4, the addition of NaCl significantly lowers the surface tension of the SME solutions. This is a typical behavior of ionic surfactant solutions [28], which is due to binding (adsorption) of counterions (Na^+) to the surfactant headgroups [29,30]. To check whether the obtained surface tension isotherms are affected by nonionic admixtures, in Fig. A4 (Appendix A) we have plotted the same data for σ, but this time versus the product $a_S a_{Na}$, where $a_S = \gamma_{\pm} C_S$ and $a_{Na} = \gamma_{\pm} C_{Na}$ are the bulk activities, respectively, of the surfactant anions and sodium cations. The activity coefficient $\gamma_{\pm}$ is calculated from the semi-empirical expression [31]

$$\log_{10}\gamma_{\pm} = bI - \frac{A\sqrt{I}}{1 + Bd_i\sqrt{I}} \tag{3}$$

originating from the Debye–Hückel theory. As before, I is the total ionic strength of the solution; d_i, A, B, and b are parameters. If I is given in moles per liter (M), the parameter values for NaCl solutions, are $A = 0.5115$ M$^{-1/2}$, $Bd_i = 1.316$ M$^{-1/2}$, and $b = 0.055$ M^{-1} at $T = 25$ °C [31]. These parameters can be used also for other 1:1 electrolytes supposedly $I < 200$ mM.

As known [32,33], for a pure ionic surfactant the surface tension isotherms measured at different concentrations of added inorganic electrolyte collapse on a single master curve when plotted as σ vs. $a_S a_{Na}$. Fig. A4 (Appendix A) shows that the data for C14- and C16-SME satisfy this requirement. In Section 4.2, the surface tension isotherms for C14- and C16-SME are fitted with an appropriate theoretical model. In contrast, similar surface tension isotherms obtained with our C12-SME sample did not satisfy the criterion in Fig. A4, which indicates that the surface tension of this sample was essentially influenced by the presence of a nonionic admixture.

4. Theoretical interpretation of surface tension

4.1. Theoretical model

An appropriate and very realistic model for theoretical interpretation of surface tension isotherms is the two-dimensional van der Waals model. The fits of data for various surfactants with this model [22,23,34,35] give excluded areas per surfactant headgroups equal to the geometrical cross-sectional areas of the headgroups determined from molecular size considerations; see e.g. Table 4 in Ref. [36]. Here, this model is applied to fit the surface tension isotherms for C14- and C16-SME in Fig. 4.

Despite the satisfaction of the criterion in Fig. A4 (Appendix A), the CMC values determined from the kinks of the surface tension isotherms in Fig. 4 are lower than those determined by conductivity measurements (Fig. 3). This difference indicates that a small amount of nonionic admixture, most probably unsulfonated methyl ester of the fatty acid, is still present. For this reason, the surface tension data were processed by using the extension of the two-dimensional van der Waals model [37] to a mixture of ionic and nonionic surfactant [22]. For convenience, the components are numbered in the same way as in Ref. [22]: 1 – ionic surfactant (SME); 2 – counterion (Na^+); 3 – inorganic coion (Cl^-), and 4 – nonionic surfactant (unsulfonated methyl ester). The two-dimensional equation of state of the considered model is [22]:

$$\sigma = \sigma_0 - \frac{kT(\Gamma_1 + \Gamma_4)}{1 - \alpha(\Gamma_1 + \Gamma_4)} + \beta(\Gamma_1 + \Gamma_4)^2 - 8kT \times \frac{I}{\kappa_D}\left[\cosh\left(\frac{\Phi_s}{2}\right) - 1\right] \tag{4}$$

where k is the Boltzmann constant, T is the temperature; Γ_1 and Γ_4 are the adsorptions (surface concentrations) of components 1 and 4;

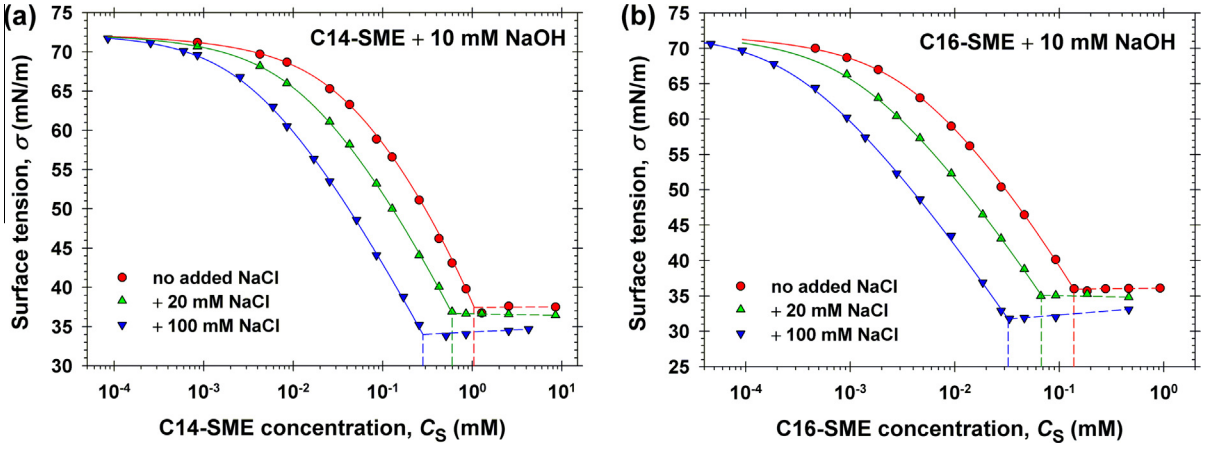

Fig. 4. Surface tension σ vs. the surfactant concentration in the presence of 10 mM NaOH; data for (a) C14-SME and (b) C16-SME at three different NaCl concentrations denoted in the figure. The kinks correspond to the CMC. The solid lines represent the best fit of the data with the theoretical model (see the text).

σ_0 is the surface tension of pure water; κ_D is the Debye screening parameter; $\Phi_s = e|\psi_s|/(kT)$ is the dimensionless surface electric potential; ψ_s is the dimensional potential; e is the elementary electric charge;

$$\alpha = \sum_{i,j=1,4} \alpha_{ij} X_i X_j, \quad \beta = \sum_{i,j=1,4} \beta_{ij} X_i X_j, \quad X_i = \frac{\Gamma_i}{\Gamma_1 + \Gamma_4} \tag{5}$$

$\alpha_{ij} = \alpha_{ji}$ and $\beta_{ij} = \beta_{ji}$ are constant parameters. In particular, α_{ij} are excluded areas per headgroup and β_{ij} are interaction parameters for the respective pairs of components at the interface [22,37]. The last term in Eq. (4) is the contribution of the diffuse part of electric double layer to the surface tension. The effect of counterion binding is taken into account by the Stern adsorption isotherm [38]:

$$\frac{\Gamma_2}{\Gamma_1 - \Gamma_2} = K_{St} \gamma_{\pm} c_2 \exp(\Phi_s) \tag{6}$$

where c_2 is the bulk concentration of counterions (Na^+), Γ_2 is their adsorption on the headgroups of the ionic surfactant; K_{St} is the Stern adsorption constant; see Appendix B. The full system of equations of the model, which is given in Appendix C, contains also the adsorption constants K_1 and K_4 of the ionic (SME) and nonionic (unsulfonated methyl ester) surface active species. The adsorption constants, K_1, K_4, and K_{St}, are related to the respective adsorption energies, E_1, E_4, and E_2, as follows [22,29]:

$$K_1 = \alpha_{11}\delta_1 \exp\left(\frac{E_1}{kT}\right), \quad K_4 = \alpha_{44}\delta_4 \exp\left(\frac{E_4}{kT}\right),$$
$$K_{St} = \alpha_{11}\delta_2 \exp\left(\frac{E_2}{kT}\right) \tag{7}$$

Here, δ_1 and δ_4 are the lengths of the respective surfactant molecules, whereas δ_2 is the counterion diameter. An additional parameter is the relative molar content of the nonionic admixture, $x_4 = c_4/c_1$, where c_1 and c_4 are the bulk concentrations of components 1 and 4 ($c_1 \equiv C_S$ at concentrations below the CMC).

4.2. Numerical results and discussion

The *binding energy*, E_2, of a Na^+ ion to the sulfonate (SO_3^-) headgroup, determined from data for the surface tension of sodium lauryl sulfonate; see Appendix B, is:

$$E_2 = 2.91kT \tag{8}$$

For the hydrated Na^+ ion, we have $\delta_2 = 0.7$ nm [39].

All parameters of the model characterize physicochemical properties of the investigated complex system: adsorption energies of the two surfactants (in an infinitely diluted adsorption layer); their excluded areas and interaction energies in the adsorption layer; the energy of counterion binding; the fraction of the nonionic admixture, etc. The values of most of these parameters are known (Appendix C). For this reason, the three experimental curves in Fig. 4a were simultaneously fitted by varying only four adjustable parameters: E_1, α_{11}, β_{11}, and x_4. The three isotherms in Fig. 4b were processed in a similar way. In both cases, the numerically minimized merit function of the least squares method has a deep minimum, which corresponds to an excellent agreement between theory and experiment. As mentioned above, all other parameters of the model are either known, or have been determined by molecular-size considerations or from expressions analogous to the Traube's rule; see Appendix C for details. The latter expressions allow one to determine the parameter values for the neighboring members of the homologous series, viz. C12-SME and C18-SME, knowing the parameters for C14- and C16-SME. The values of all parameters for C*n*-SME ($n = 12, 14, 16, 18$) are summarized in Table 1.

Table 1
Adsorption parameters of C*n*-SME, $n = 12$, 14, 16 and 18.

Surfactant	α_{11} (Å^2)	K_1 (M^{-1})	δ_1 (Å)	$E_1/(kT)$	$\widehat{\beta}_{11}$
C12-SME	37.0	5.916×10^{4}[b]	22.3	11.69[a]	1.47[a]
C14-SME	37.0	5.745×10^{5}	24.8	13.85	1.74
C16-SME	37.0	5.543×10^{6}	27.4	16.02	1.98
C18-SME	37.0	5.282×10^{7}[b]	29.9	18.19[a]	2.24[a]

[a] Extrapolated values for energy of adsorption and interaction parameter.
[b] Calculated values for the adsorption constant.

In practice, C*n*-SME always contains a small admixture of unsulfonated methyl ester of the fatty acid, C*n*-ME. The chemical structure of C*n*-ME is very similar to that of the respective protonated fatty acid, with the only difference that –H is replaced by $–CH_3$ in the headgroup. For this reason, we could expect that the adsorption parameters for C*n*-ME are very close to those for the fatty acid, HC*n*, with the same hydrocarbon tail. Correspondingly, in our calculations and in the data fits for C*n*-ME we have used the adsorption parameters for HC*n* from Ref. [40]. All adsorption parameters related to C*n*-ME are summarized in Table 2. In the calculations, it is convenient to use the dimensionless interaction parameters:

$$\widehat{\beta}_{11} = \frac{2\beta_{11}}{\alpha_{11}kT}, \quad \widehat{\beta}_{14} = \frac{2\beta_{14}}{\alpha_{11}kT}, \quad \widehat{\beta}_{44} = \frac{2\beta_{44}}{\alpha_{44}kT} \tag{9}$$

The following relations have also been used [22]:

$$\widehat{\beta}_{14} = \widehat{\beta}_{11}\left(\frac{\alpha_{11}}{\alpha_{14}}\right)^{3/2}, \quad \alpha_{14} = \left(\frac{\sqrt{\alpha_{11}} + \sqrt{\alpha_{44}}}{2}\right)^2 = 29.4\ \text{Å}^2 \tag{10}$$

(see Tables 1 and 2). Because at 25 °C the fatty acids with $n \geqslant 12$ carbon atoms undergo a surface phase transition, we have set $\widehat{\beta}_{44} = 6.75$ (for $n \geqslant 12$). This value corresponds to the phase transition in the van der Waals model. Further details can be found in Appendix C.

It should be noted that the excluded area per SME headgroup, $\alpha_{11} = 37$ Å^2 (Table 1), which has been determined from the best fit of the data in Fig. 4, coincides with the cross-sectional area of the sulfonate group. Indeed, from the radius 3.43 Å of the hydrated sulfonate ion (Appendix B), we calculate $\pi \times (3.43)^2 = 36.96$ nm^2 ≈ 37 Å^2. The large diameter of the hydrated sulfonate group, 6.86 Å (that contributes to the molecular length), is the reason of the greater values of δ_1 in Table 1, as compared to δ_4 in Table 2. The smaller values of E_1 in Table 1, as compared to E_4 in Table 2 (with the same n), can be explained with the location of the sulfonate group before the carboxylic group (Fig. 1). Substituting E_2 from Eq. (8) and α_{11} from Table 1, from Eq. (7) we find the Stern constant:

$$K_{St} = 2.86\ \text{M}^{-1}\ (\text{for } Na^+ \text{ to C}n\text{-SME}) \tag{11}$$

It should also be noted that in semi-logarithmic scale, the data for K_1 and K_4 in Tables 1 and 2 excellently comply with linear dependences in agreement with the Traube's rule (see Fig. C1 in Appendix C):

$$\log_{10}K_1 = -1.128 + 0.4918n \tag{12}$$

$$\log_{10}K_4 = -0.750 + 0.4688n \tag{13}$$

Using the parameter values from Table 1 and the theoretical model, one can calculate various properties of the adsorption layers from *pure* C*n*-SME ($x_4 = 0$): surface tension isotherms; adsorption Γ_1; degree of counterion binding (occupancy of the Stern layer) Γ_2/Γ_1, and surface electric potential ψ_s, see Fig. 5. The computational procedure is described in Appendix C and Refs. [22,29].

In Fig. 5a, the value of σ at the CMC is $\approx$39 mN/m, which is a typical value for pure ionic surfactants at the CMC. The value of the adsorption at CMC is $\Gamma_1 \approx 3.4$ μmol/m^2, but for C18-SME this

Table 2
Adsorption parameters related to C*n*-ME, n = 12, 14, 16 and 18.

Molecule	α_{44} (Å^2)	K_4 (M^{-1})	δ_4 (Å)	$E_4/(kT)$	$\widehat{\beta}_{14}$	x_4 (%)
C12-ME	22.6	7.450×10^4	19.6	12.54	2.08	–
C14-ME	22.6	6.555×10^5	22.2	14.59	2.46	0.017[a]
C16-ME	22.6	5.665×10^6	24.7	16.64	2.80	0.010[a]
C18-ME	22.6	4.846×10^7	27.2	18.69	3.17	–

[a] Specific values determined from fits of the data in Fig. 4.

value is reached at c.a. two orders of magnitude lower concentration as compared with C12-SME (Fig. 5b). The degree of counterion binding, Γ_2/Γ_1, increases with the rise of C_S and approaches 0.8 near the CMC (Fig. 5c). The magnitude of the surface potential, $-\psi_s$, increases with the rise of n. The difference between two curves in Fig. 5d is ≈40 mV. This difference is related to the fact that the surfactant of longer hydrocarbon chain forms denser adsorption layers at lower surfactant concentrations, at which the Debye screening of the electric field is weaker. The maximum in the $|\psi_s|$ vs. C_S curve is typical for ionic surfactant solutions without added salt [22,29,30]. This maximum is due to the fact that at the lower C_S the potential $|\psi_s|$ increases because of the rise of the surface charge density (upon the increase of surfactant adsorption), whereas at the higher C_S the Debye screening prevails and $|\psi_s|$ begins to decrease.

As already mentioned, the surface tension isotherms in Fig. 4 are affected by the presence of a small amount of nonionic surface active admixture, supposedly unsulfonated methyl ester (C*n*-ME). From the fits of the data we determined x_4 = 0.017% and 0.010% for the nonionic admixture of C14- and C16-ME in C14- and C16-SME, respectively. These values of x_4 are very low, but nevertheless, the nonionic admixture (component 4) affects the properties of the adsorption layers. Its effect is visible in Fig. 6a and b, where Γ_4 becomes essential near the CMC. Γ_4 reaches slightly greater values for C14-SME (as compared to C16-SME) because of the greater x_4 = 0.017% (as compared to 0.010%).

In Fig. 6c and d, the degree of counterion binding, Γ_2/Γ_1, is markedly higher than in Fig. 5c, which is due to the higher concentrations of Na^+ counterions from the added NaOH and NaCl. Moreover, Γ_1 is also greater at higher electrolyte concentrations, which is due to the screening of the electrostatic repulsion between the SME anions and the like-charged interface, as well as between the adsorbed SME anions. As is should be expected, the increased Debye screening significantly decreases the magnitude of the surface electric potential – compare Figs. 6e and f with 5d.

The calculated dependences in Fig. 6 correspond to the SME samples used in the present study, which contain specific amounts of nonionic admixture, characterized by the values of x_4. However, the methodology described here and the parameter values in Tables 1 and 2 would allow one to determine x_4 also for other SME samples and to characterize the properties of their adsorption layers by dependencies analogous to those in Fig. 6. The computational procedure is described in Appendix C and Ref. [22].

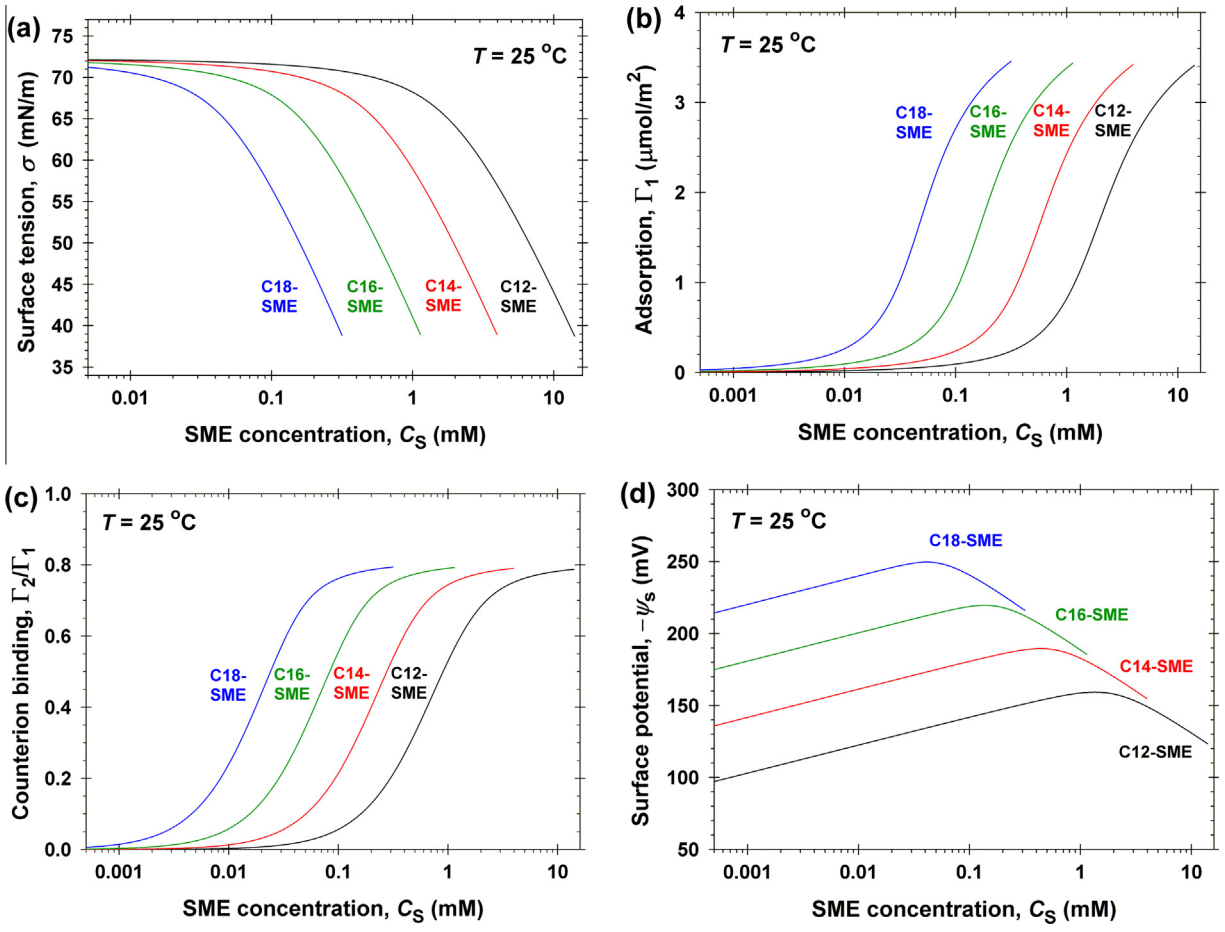

Fig. 5. Properties of the surfactant adsorption layers from *pure* C*n*-SME for n = 12, 14, 16 and 18 at the air/water interface, calculated using the parameter values in Table 1. (a) Surface tension, σ, vs. C_S; (b) surfactant adsorption, Γ_1, vs. C_S; (c) degree of counterion binding, Γ_2/Γ_1, vs. C_S; (d) magnitude of the surface electric potential, $-\psi_s$, vs. C_S. All curves end at the CMC.

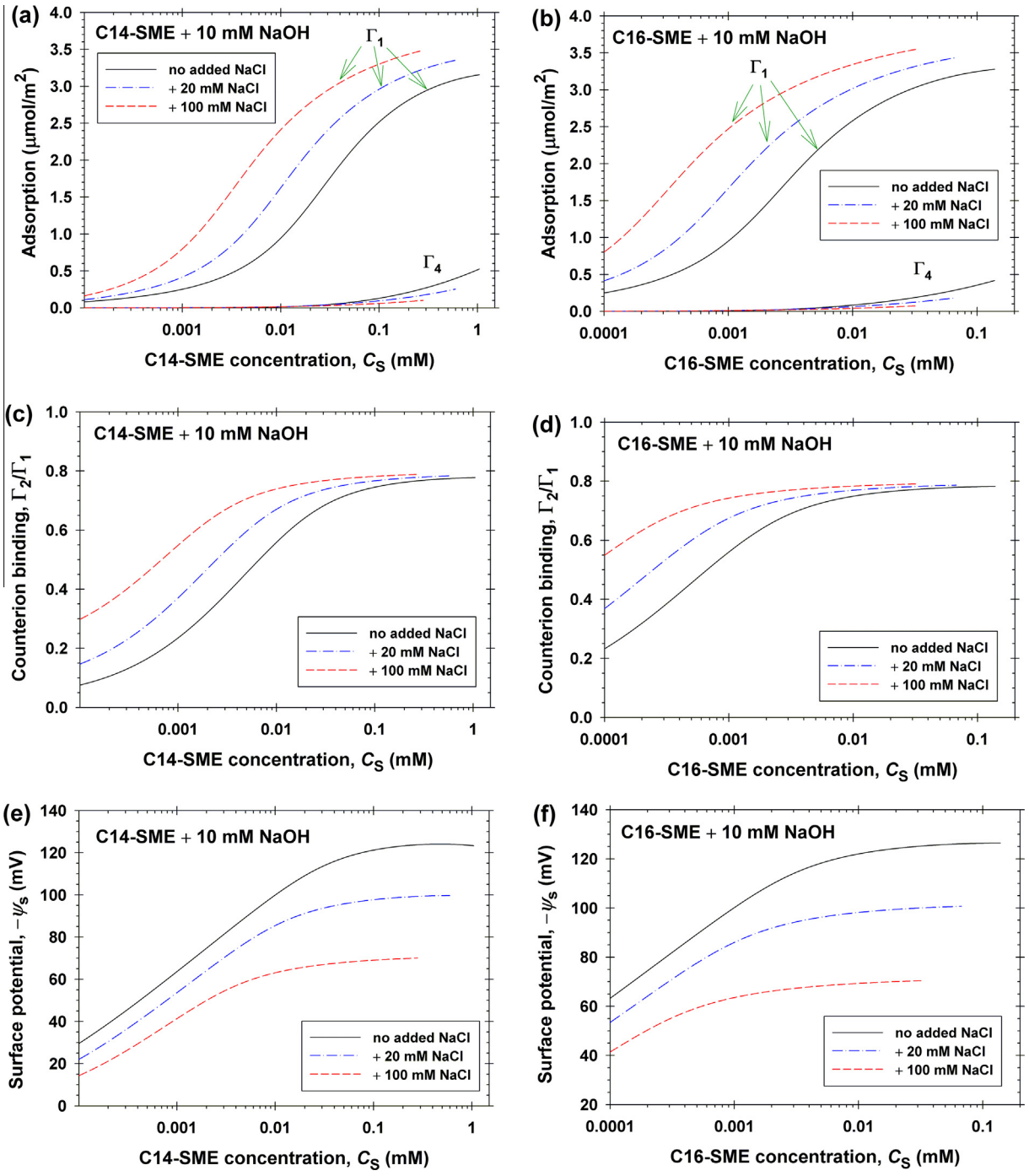

Fig. 6. Calculated concentration dependences of the properties of adsorption layers of the C14- and C16-SME solutions, for which σ- vs. -C_S isotherms are shown in Fig. 4. These SME samples contain a small nonionic admixture (component 4) – see x_4 in Table 2. (a and b) Adsorptions, Γ_1 and Γ_4 vs. C_S. (c and d) Degree of counterion binding, Γ_2/Γ_1, vs. C_S. (e and f) Magnitude of the surface electric potential, $-\psi_s$, vs. C_S. All curves end at the CMC.

Finally, it should be mentioned that some authors [41,42] called into question the applicability of the Gibbs equation to the case of adsorption layers from ionic surfactants. As demonstrated in Refs. [29,43], the problem can be solved by including the counterion binding in the Gibbs equation. Then, the Gibbs equation, presented by its corollary, Eq. (4), becomes a part of a system of equations, which includes the theory of the electric double layer; see Appendices B and C. In the case of counterion binding to the surface of micelles, the problem was addressed in Ref. [27].

5. Micellization in SME solutions

5.1. Dependence of CMC on the concentration of added NaCl

The dependence of the CMC on the concentration of counterions, varied by the addition of inorganic electrolyte allows one to determine the surfactant micellization parameters, which can be further employed to predict various properties of the micellar solutions; see Ref. [27] for details.

As demonstrated in Section 3.1, the value of CMC determined by electrical conductivity measurements is insensitive to the presence of small amounts of nonionic admixture, so that the CMC values obtained in this way can be regarded as those of the pure ionic surfactant ($x_4 = 0$) in the presence of a small NaCl admixture (see above). In Fig. 7, the CMC values obtained by conductivity for C12-, C14- and C16-SME are shown by triangles. In contrast, the CMC determined by surface-tension measurements is extremely sensitive to nonionic admixtures. The circles in Fig. 7b and c represent the CMC values determined from the surface-tension isotherms in Fig. 4a and b, where the molar fraction of the nonionic admixture (relative to SME), determined from the fit of the surface tension data, is $x_4 = 0.017\%$ and 0.010%, respectively, for C14- and C16-SME; see Table 2; more details can be found in Appendix D. The difference between the CMC values determined by conductivity and surface tension measurements allows one to find the solubilization constant, $K_4^{(mic)}$, of the nonionic admixture (supposedly C*n*-ME) in the micelles of SME; see Section 5.2.

In Fig. 7a, the data have been obtained by *conductivity* measurements, so that they can be considered as representative for the pure C12-SME ($x_4 = 0$). The concentration on the abscissa is that of the added NaCl. CMC values determined by surface tension measurements are absent in Fig. 7a, because the surface tension isotherms of the used C12-SME sample (unlike those in Fig. 4) exhibit a minimum in the CMC region.

In Fig. 7b and c, the CMC values obtained by *conductivity* for C14- and C16-SME are plotted vs. the concentration of sodium due to the added NaCl. The respective CMC data obtained by *surface tension* measurements are plotted vs. the sodium concentration due to both added NaCl and NaOH; see Fig. 4.

In Fig. 7d, the CMC data obtained by *conductivity*, together with the respective theoretical fits, are plotted in double logarithmic scale vs. the total counterion (Na) concentration. The obtained curves can be described well with a linear dependence, as first established by Corrin and Harkins [44] for ionic surfactants. The total counterion concentration, C_{Na} takes into account also the contribution of the electrolyte admixture in the SME sample; see the last two paragraphs of Section 3.2. The three straight lines in Fig. 7d are practically parallel. The calculated slopes of the ln(CMC) versus ln(C_{Na}) are −0.773 (C12-SME), −0.781 (C14-SME), and −0.788 (C16-SME).

5.2. Theoretical modeling of micellization

The chemical equilibrium between micelles and monomers in mixed solutions of ionic and nonionic surfactant, and the effect of counterion binding are described by the following four equations [27]:

$$\ln(c_1\gamma_{\pm}) = \ln K_1^{(mic)} + \ln(y_1) + \Phi_s \tag{14}$$

$$\ln(c_{12}) = \ln K_1^{(mic)} + \ln(y_2) \tag{15}$$

$$\ln(c_4) = \ln K_4^{(mic)} + \ln(y_4) \tag{16}$$

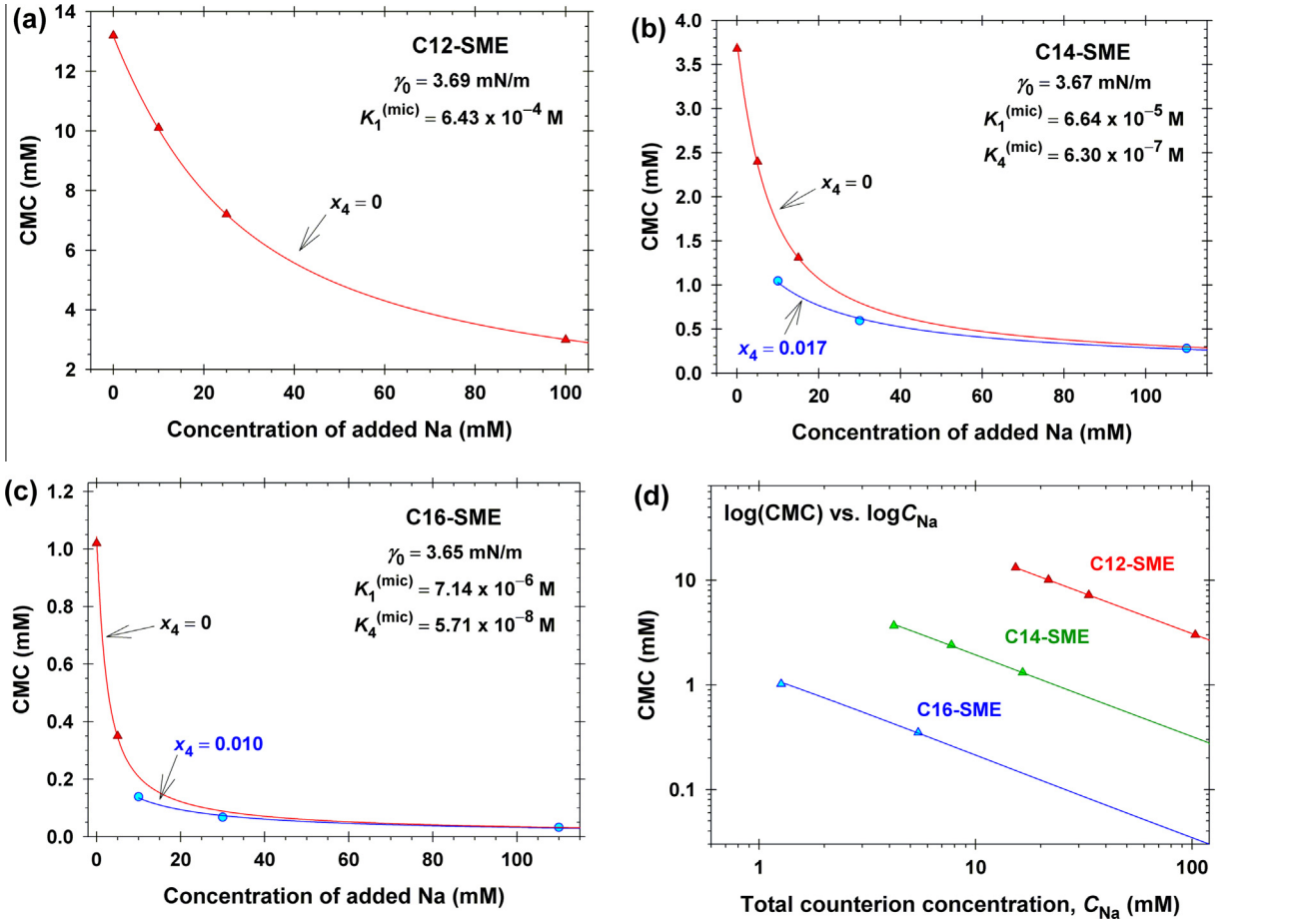

Fig. 7. CMC of (a) C12-SME; (b) C14-SME, and (c) C16-SME vs. the concentration of added Na. (d) Double-log plot of the CMC vs. the total counterion concentration (from both SME and added salt), C_{Na}, for pure SMEs ($x_4 = 0$). Δ – CMC determined by electrical conductivity, which corresponds to pure SME; ○ – CMC determined by surface tension, which is affected by the fraction of the nonionic admixture, x_4. The solid lines are fits with the theoretical model in Section 5.2; the parameter values determined from the fits are shown in the figures.

$$c_{12} = K_{St} c_1 c_2 \gamma_{\pm}^2 \tag{17}$$

Eqs. (14)–(16) follow from the equality of the (electro)chemical potentials of the monomers in the bulk and in the micelles for the respective components; c_1, c_{12} and c_4 are the bulk monomer concentrations, respectively, of the surfactant ion (C*n*-SME$^-$), of the surfactant ion with bound counterion (loose solvent-shared (hydrated) ion pair, rather than a chemical bond), and of the nonionic surface active component (unsulfonated methyl ester, C*n*-ME). Correspondingly, y_1, y_2 and y_4 are the molar fractions of these components in the micelles ($y_1 + y_2 + y_4 = 1$). There is no binding of Cl^- coions ($y_3 = 0$). Because components 1 (ionic surfactant) and 4 (nonionic admixture) have similar hydrocarbon chains, the micelle is considered as an ideal mixture of these components, and correspondingly, activity coefficients are missing in the right-hand sides of Eqs. (14)–(16). As a rule, the micellar activity coefficients are different from 1 if there is a mismatch between the hydrocarbon chains of the two components with more than two CH_2 groups [45,46]. The micellization constants $K_1^{(mic)}$ and $K_4^{(mic)}$ are related to the (non-electrostatic) work for transfer of a molecule of the respective component from monomeric form in the bulk water solution into the micelle:

$$kT \ln K_i^{(mic)} = \mu_i^{(mic,0)} - \mu_i^{(w,0)}, \quad i = 1, 4 \tag{18}$$

where $\mu_i^{(w,0)}$ and $\mu_i^{(mic,0)}$ are the standard chemical potentials of this molecule in the water and in the micelles, respectively. As before, $\Phi_s = e|\psi_s|/(kT)$ is the dimensionless surface electric potential, but this time it refers to the surface of the micelle. Eq. (17) expresses the association–dissociation equilibrium between surfactant ions and counterions in the bulk; c_2 is the bulk counterion concentration. K_{St} is the Stern constant of counterion binding, which takes the same value as for the surfactant adsorption layer at the solution's surface [27]; see Eq. (11). Indeed, if Eq. (14) is subtracted from Eq. (15), and c_{12} is eliminated from Eq. (17), we obtain the Stern isotherm in its form for a surfactant micelle:

$$\frac{y_2}{y_1} = K_{St} \gamma_{\pm} c_2 \exp(\Phi_s) \tag{19}$$

– compare with Eq. (6). To close the system of equations and to determine Φ_s, one needs an additional equation, which originates from the electric double layer theory [27]:

$$(1 - y_4)\gamma_0 = 4kT \left(\frac{2I}{\pi L_B}\right)^{1/2} \left\{ \sinh^2\left(\frac{\Phi_s}{4}\right) + \frac{2}{\kappa_D R_m} \ln\left[\cosh\left(\frac{\Phi_s}{4}\right)\right] \right\} \tag{20}$$

As before, I is the solution's ionic strength; $\kappa_D = (8\pi L_B I)^{1/2}$ is the Debye screening parameter; $L_B = e^2/(4\pi\varepsilon_0\varepsilon kT)$ is the Bjerrum length; ε_0 is the dielectric permittivity of vacuum and ε is the dielectric constant of the solvent (water); $L_B = 0.72$ nm for water at 25 °C; R_m is the micelle radius at the level of the surface charges; γ_0 is a constant parameter (non-electrostatic component of the micelle surface tension) that characterizes a given ionic surfactant. Eq. (20) was first derived by Mitchell and Ninham [47] for single-component micelles and states that the repulsive electrostatic surface pressure due to the ionized surfactant headgroups is counterbalanced by the attraction (van der Waals and hydrophobic) between the molecules in the micelle. The full system of equations of the model, which includes also some mass balance equations, and the numerical procedure can be found in Appendix E and Ref. [27].

In summary, the considered micellization model characterizes the nonionic component with a single micellization parameter, $K_4^{(mic)}$. In contrast, the ionic component is characterized by three micellization parameters: $K_1^{(mic)}$, γ_0 and K_{St}. For the considered experimental systems, these parameters can be determined as explained in Section 5.3.

5.3. Micellization parameters and numerical results

As already mentioned, K_{St} is known from the fits of the surface-tension data; see Eq. (11). The micelle radius, which enters Eq. (20), was set equal to the length of the surfactant molecule, $R_m = \delta_1$; see Table 1. The data for CMC of C12-SME in Fig. 7a were fitted with the theoretical model from Section 5.2 and two micellization parameters of this surfactant, $K_1^{(mic)}$ and γ_0, have been determined. In Fig. 7b and c, the experimental curves with $x_4 = 0$ and $x_4 \neq 0$ have been simultaneously fitted with the model, and three parameters have been determined from the fit: $K_1^{(mic)}$, γ_0, and $K_4^{(mic)}$. In particular, $K_4^{(mic)}$ accounts for the difference between the curve with $x_4 \neq 0$ from that with $x_4 = 0$. The values of x_4 determined from the surface tension data (see Table 2) have been used. The parameter values determined from the fits are shown in Table 3.

The binding constant of the Na^+ counterion to the sulfonate headgroup of C*n*-SME, K_{St}, is not expected to depend on the chain-length, *n*. The values of γ_0 obtained from the fits are close to the values for other surfactants in Table 3 of Ref. [27]. The obtained values of $K_1^{(mic)}$ excellently comply with a straight line, when plotted as $\log_{10} K_1^{(mic)}$ vs. *n*; see Fig. 8. This dependence is an analogue of the Traube's rule for surfactant adsorption. For comparison, in Fig. 8 we have plotted also data from Ref. [45] for the micellization (solubilization) constant, $K_A^{(mic)}$, of protonated fatty acids (HC*n*) in micellar solutions of cocamidopropyl betaine (CAPB) and sodium laurylethersulfate with one ethylene-oxide group (SLES). As seen in the figure, the slopes of the lines for C*n*-SME and HC*n* are very close. In Fig. 8, the two values for $K_4^{(mic)}$ from Fig. 7b and c are fitted with a straight line of the same slope as for the fatty acids. The equations of the straight lines in Fig. 8 are:

$$\log_{10} K_1^{(mic)} = 2.668 - 0.4885n \tag{21}$$

$$\log_{10} K_A^{(mic)} = 1.615 - 0.4985n \tag{22}$$

$$\log_{10} K_4^{(mic)} = 0.7555 - 0.4985n \tag{23}$$

In Table 3, the values of $K_1^{(mic)}$ and $K_4^{(mic)}$ for $n = 18$, as well as the value of $K_4^{(mic)}$ for $n = 12$, have been obtained from Eqs. (21) and (23), i.e. by extrapolation. The smaller intercept in Eq. (23), as compared with that in Eq. (22), corresponds to the fact that the methyl ester of a given fatty acid is more hydrophobic than the fatty acid, itself. By absolute value, the slope coefficients in Eqs. (21) and (23) are close to the slope coefficients in the analogous dependences for the adsorption constants at the air/water interface; see Eqs. (12) and (13).

At known micellar constants K_{St}, γ_0 and $K_1^{(mic)}$ (see Table 3), the model from Section 5.2 enables one to predict various properties of the micellar solutions of C*n*-SME. As an illustration, Fig. 9a–c show plots of c_1, c_2 and c_{mic} vs. the total surfactant concentration, C_S, for pure C12-, C14- and C16-SME without nonionic and salt

Table 3
Micellar parameters of pure C*n*-SME (CMC, K_{St}, γ_0, $K_1^{(mic)}$) and C*n*-ME ($K_4^{(mic)}$).

n	CMC (mM)	K_{St} (M^{-1})	γ_0 (mN/m)	$K_1^{(mic)}$ (M)	$K_4^{(mic)}$ (M)
12	14.1	2.86	3.69	6.43×10^{-4}	5.94×10^{-6}[a]
14	3.98	2.86	3.67	6.64×10^{-5}	6.30×10^{-7}
16	1.14	2.86	3.65	7.14×10^{-6}	5.71×10^{-8}
18	0.32[a]	2.86	3.63[a]	7.48×10^{-7}[a]	6.06×10^{-9}[a]

[a] Extrapolated values.

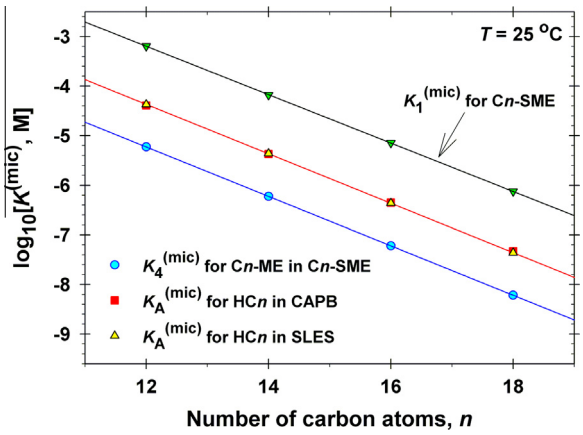

Fig. 8. Plots of $\log_{10}K^{(mic)}$ vs. n. The data for the micellar constants of Cn-SME and Cn-ME, $K_1^{(mic)}$ and, $K_4^{(mic)}$ are from Table 3, whereas the data for the respective constant for fatty acids incorporated in CAPB and SLES micelles, $K_A^{(mic)}$, are from Table B.2 in Ref. [45]. The straight lines correspond to Eqs. (21)–(23).

admixtures. As before, c_1 and c_2 are, respectively, the concentrations of free surfactant monomers and Na^+ counterions; c_{mic} is the concentration of surfactant molecules incorporated in micelles. By definition, $c_{mic} \equiv 0$ for $C_S \leqslant$ CMC. As seen in Fig. 9a–c, above the CMC, c_{mic} strongly increases and becomes equal to c_1 around $C_S \approx 1.7 \times$ CMC. In other words, for $C_S > 1.7 \times$ CMC, most of the surfactant molecules are incorporated in micelles. In addition, above the CMC c_1 decreases, but c_2 increases. The increase of c_2 is due to counterions dissociated from the micelles (whose concentration increases). In turns, the rise of c_2 enhances the Debye screening and counterion binding, both of them leading to decrease of the magnitude of the surface electric potential $-\psi_s$; see Fig. E1c in Appendix E. Finally, in accordance with Eq. (14) the decrease of $\Phi_s = e|\psi_s|/(kT)$, and of y_1, as well, leads to a decrease in the concentration of surfactant monomers, c_1, as seen in Fig. 9a–c. Qualitatively, the plots for C12-, C14- and C16-SME in Fig. 9a–c seem similar, but the concentration ranges along both coordinate axes correspond to lower concentrations at greater n values.

Fig. E1c in Appendix E shows plots of the magnitude of the micelle surface electric potential, $-\psi_s$, vs. C_S, for Cn-SME, $n = 12$, 14, 16 and 18, predicted by the model. One sees that the micelle surface potential is the highest for C18-SME. This could be explained with the fact that at $n = 18$ the counterion concentration, c_2, is the lowest (compare Fig. 9a and c), and correspondingly, the Debye screening of the electric field is the weakest. The calculated degree of counterion binding to the surfactant headgroups at the micelle surface, y_2, takes close values for all investigated chain-lengths ($n = 12$–18), and increases from 0.37 at the CMC of C18-SME (0.3157 mM) to ≈0.77 at $C_S = 100$ mM for all chain-lengths; see Fig. E1d in Appendix E.

The model from Section 5.2 enables one to predict the CMC of ionic surfactants – this is the intersection point of the theoretical curve c_{mic} vs. C_S with the horizontal axis ($c_{mic} = 0$); see Fig. 9a–c. The calculated values of CMC of pure Cn-SME vs. n are listed in Table 3 and plotted in Fig. 9d. One sees that ln(CMC) is a linear

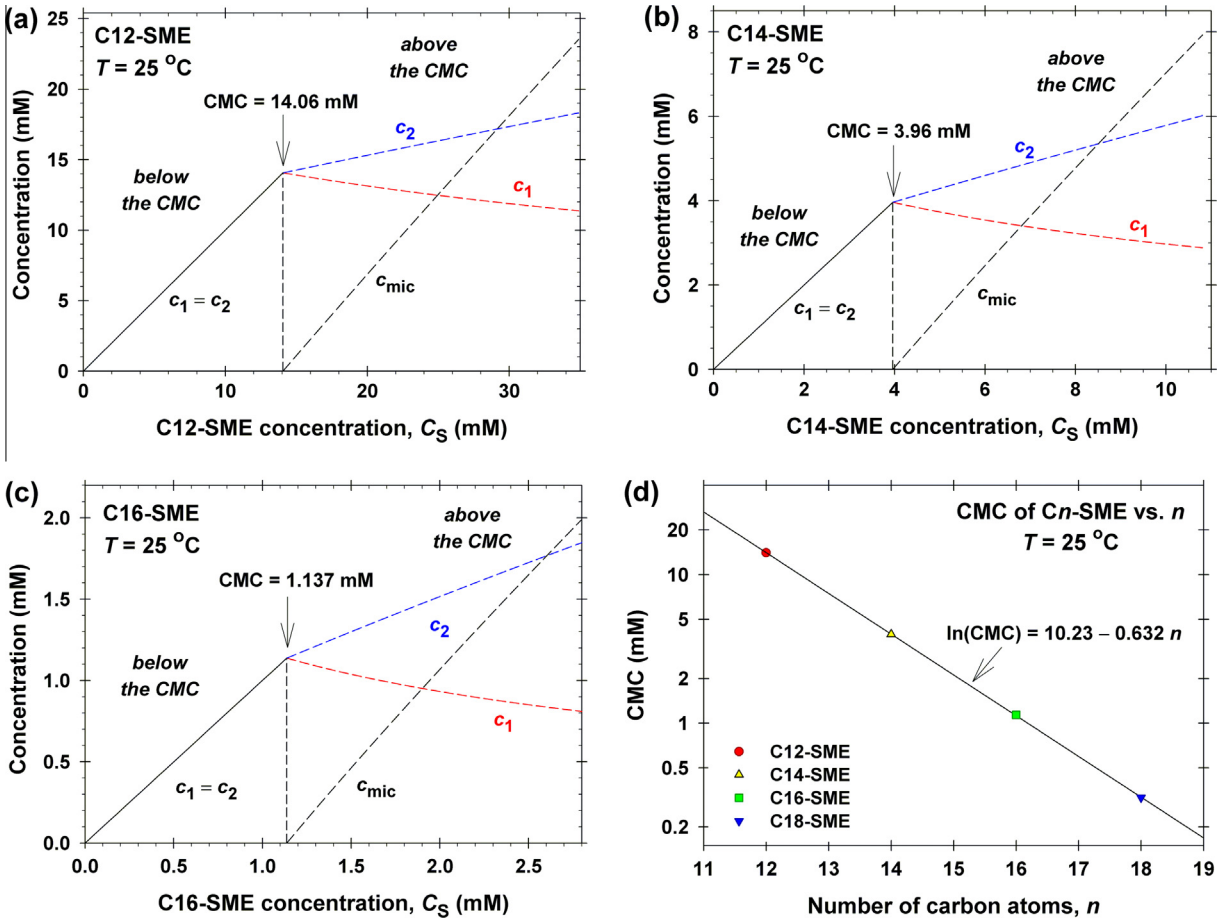

Fig. 9. Plots of the concentrations of free surfactant monomers, c_1, free counterions, c_2, and surfactant molecules incorporated in micelles, c_{mic}, vs. the total surfactant concentration, C_S: (a) C12-SME; (b) C14-SME, and (c) C16-SME. (d) Plot of the CMC of pure Cn-SME as a function of n (see Table 3).

function of n with slope −0.632. Such linear dependence is typical for the surfactants, as illustrated in Fig. D1 in Appendix D for alkyltrimethylammonium bromides (C_nTAB).

Combining the results in Figs. 7d and 9d, we obtain the following empirical expression:

$$\ln(\mathrm{CMC}) = 18.21 - 1.125n - 0.781\ln(C_{\mathrm{Na}}) \quad (24)$$

for the prediction of the CMC of pure Cn-SME as a function of the chain length, n, and the total concentration of sodium counterions, C_{Na}. In Eq. (24), CMC and C_{Na} are expressed in mM. In the absence of added salt, one has to substitute C_{Na} = CMC for the counterions dissociated from the SME.

6. Summary and conclusions

Here, we present a quantitative characterization of sulfonated methyl esters, Cn-CME for n = 12, 14, 16 and 18 by determining their CMCs, surface tension isotherms at the air/water interface; physicochemical parameters of adsorption and micellization, which further enable one to predict the surfactant adsorption, degree of counterion binding, surface electric potential, and the effect of nonionic additives (methyl esters of the fatty acids).

A key for quantitative data interpretation is the experimental fact that the CMC of ionic surfactants determined by conductivity is insensitive to the presence of a nonionic surface-active additive. This is demonstrated with the addition of dodecanol to SDS solutions. Up to 6 mol% (relative to SDS), the dodecanol does not produce any effect on the measured conductivity (Fig. 2), although it strongly affects the solution's surface tension. For this reason, the CMC values determined by conductivity can be regarded as the CMC of the pure Cn-SME. Because the CMC values determined by surface-tension measurements are lower than those determined by conductivity, we conclude that the investigated ionic-surfactant samples contain nonionic admixtures. For this reason, physicochemical characteristics of SMEs, such as surface tension isotherms and critical micelle concentrations, published in the literature often differ, sometimes up to order of magnitude in the CMC values [3,14–21]. The method developed in the present article allowed us to determine the surface tension isotherms and the CMCs of the pure sulfonated methyl esters.

The measurements of the surface tension of SME solutions at three different NaCl concentrations (Fig. 4), and the fit of the data by means of the two-component van der Waals model [22], allowed us to find the adsorption parameters of Cn-SME (Table 1) and of the small nonionic admixture, supposedly unsulfonated methyl ester of the fatty acid, Cn-ME (Table 2), including the fraction, x_4, of this admixture.

Furthermore, the fit of the data for the solution's CMC (measured by conductivity and surface tension) by the generalized phase-separation model of micellization [27], allowed us to determine the micellar parameters of the ionic surfactant, γ_0 and, $K_1^{(\mathrm{mic})}$ and of the nonionic admixture, $K_4^{(\mathrm{mic})}$. Having determined the parameters of the (pure) ionic surfactant one can predict its interfacial properties, surface tension, adsorption, degree of counterion binding, surface electric potential (see Fig. 5), as well as the properties of its micellar solutions; see Fig. 9 and Fig. E1 in Appendix E. The properties of the solutions of the basic surfactant (Cn-SME) with different amounts of nonionic admixture (Cn-ME) can be also predicted; see Fig. 6 and Fig. E3.

In this way, using Cn-SME as an example, we have demonstrated the application of a new and powerful method, called (for brevity) *computer purification* of ionic surfactants. Practically, most samples of commercially available ionic surfactants contain small nonionic admixtures that, however, might strongly affect their adsorption and micellization properties (e.g. the CMC). It is very difficult, and in some cases – impossible, to purify the ionic surfactant from these admixtures. For this reason, in practical applications the ionic surfactants are often used without any purification. However, as demonstrated in this paper, the purification can be carried out by computer fits of an appropriate set of data from conductivity and surface-tension measurements using a quantitative physicochemical model in terms of generally accepted chemical-equilibrium and mass-balance equations. In this way, one can obtain, e.g., the surface tension of the purified surfactant (see Fig. 5a), which otherwise would demand considerable experimental efforts. The method of computer purification can be applied to any ionic surfactant, if there is information about the chemical nature of the nonionic admixture. The computer purification has the potential to become a basic method for the quantitative analysis and computer modeling of the properties of solutions from ionic surfactants, alone or in mixtures with other surface-active substances.

Acknowledgments

The authors gratefully acknowledge the support from KLK OLEO and from the COST Action CM1101. The C12 and C14 samples have been kindly provided by Dr. Hazimah Abu Hassan from MPOB. The authors thank Dr. Lilia Vinarova and Ms. Lydia Dimitrova for their help in the analysis of surfactant samples.

Appendix A. Supplementary material

Supplementary data associated with this article can be found, in the online version, at http://dx.doi.org/10.1016/j.jcis.2015.07.020.

References

[1] M.J. Rosen, Surfactants and Interfacial Phenomena, third ed., John Wiley & Sons, Hoboken, New Jersey, 2004.
[2] T. Germain, in: F.E. Friedly (Ed.), Surface Science Series, vol. 98, Marcel Dekker, New York, 2001, pp. 117–144.
[3] T. Satsuki, INFORM 3 (1992) 1099–1105.
[4] T. Satsuki, K. Umehara, Y. Yoneyama, J. Am. Oil Chem. Soc. 69 (1992) 672–677.
[5] R. Ghazali, S. Ahmad, J. Oil Palm Res. 16 (2004) 39–44.
[6] L. Cohen, F. Trujillo, J. Surf. Deterg. 1 (1998) 335–341.
[7] L. Cohen, F. Trujillo, J. Surf. Deterg. 2 (1999) 363–365.
[8] L. Cohen, F. Soto, M.S. Luna, J. Surf. Deterg. 4 (2001) 147–150.
[9] L. Cohen, F. Soto, A. Melgarejo, D.W. Roberts, J. Surf. Deterg. 11 (2008) 181–186.
[10] L. Cohen, D.W. Roberts, C. Pratesi, Chem. Eng. Trans. 21 (2010) 1033–1038.
[11] L. Cohen, D.W. Roberts, C. Pratesi, in: E.T. Hagen (Ed.), Detergents: Types, Components and Uses, Nova Science Publishers, New York, 2011, pp. 121–142.
[12] P. Siwayanan, R. Aziz, N.A. Bakar, H. Ya, R. Jokiman, S. Chelliapan, J. Surf. Deterg. 17 (2014) 871–880.
[13] P. Siwayanan, R. Aziz, N.A. Bakar, H. Ya, R. Jokiman, S. Chelliapan, J. Oleo Sci. 63 (2014) 585–592.
[14] M. Luo, Z. Jia, H. Sun, L. Liao, Q. Wen, Colloids Surf. A 395 (2012) 267–275.
[15] M. Fujiwara, T. Okano, T.-H. Nakashima, A.A. Nakamura, G. Sugihara, Colloid Polym. Sci. 275 (1997) 474–479.
[16] S.R. Patil, T. Mukaiyama, A.K. Rakshit, J. Surf. Deterg. 7 (2004) 87–96.
[17] W.H. Lim, R.A. Ramle, J. Dispersion Sci. Technol. 30 (2009) 131–136.
[18] S.P. Wong, W.H. Lim, S.F. Cheng, C.H. Chuan, J. Oil Palm Res. 23 (2011) 968–973.
[19] S.P. Wong, W.H. Lim, S.-F. Cheng, C.H. Chuan, J. Surf. Deterg. 15 (2012) 601–611.
[20] A.J. Stirton, R.G. Bistline, J.K. Weil, W.C. Ault, E.W. Maurer, JAOCS 39 (1962) 128–131.
[21] A.J. Stirton, JAOCS 39 (1962) 490–496.
[22] P.A. Kralchevsky, K.D. Danov, V.L. Kolev, G. Broze, A. Mehreteab, Langmuir 19 (2003) 5004–5018.
[23] K.D. Danov, S.D. Kralchevska, P.A. Kralchevsky, G. Broze, A. Mehreteab, Langmuir 19 (2003) 5019–5030.
[24] K. Tajima, M. Muramatsu, T. Sasaki, Bull. Chem. Soc. Jpn. 43 (1970) 1991–1998.
[25] A.A. Ravdel, A.M. Ponomareva, Concise Handbook of Physicochemical Quantities, eigth ed., Khimiya, Leningrad, 1983 (in Russian).
[26] P.A. Kralchevsky, M.P. Boneva, K.D. Danov, K.P. Ananthapadmanabhan, A. Lips, J. Colloid Interface Sci. 327 (2008) 169–179.
[27] K.D. Danov, P.A. Kralchevsky, K.P. Ananthapadmanabhan, Adv. Colloid Interface Sci. 206 (2014) 17–45.

[28] K. Tajima, Bull. Chem. Soc. Jpn. 44 (1971) 1767–1771.
[29] P.A. Kralchevsky, K.D. Danov, G. Broze, A. Mehreteab, Langmuir 15 (1999) 2351–2365.
[30] V.L. Kolev, K.D. Danov, P.A. Kralchevsky, G. Broze, A. Mehreteab, Langmuir 18 (2002) 9106–9109.
[31] R.A. Robinson, R.H. Stokes, Electrolyte Solutions, second ed., Dover, Ney York, 2002.
[32] V.B. Fainerman, D. Möbius, R. Miller, Surfactants: Chemistry, Interfacial Properties, Applications, Elsevier, Amsterdam, 2001.
[33] V.B. Fainerman, E.H. Lucassen-Reynders, Adv. Colloid Interface Sci. 96 (2002) 295–323.
[34] D.S. Valkovska, G.C. Shearman, C.D. Bain, R.C. Darton, J. Eastoe, Langmuir 20 (2004) 4436–4445.
[35] K.D. Danov, S.D. Kralchevska, P.A. Kralchevsky, K.P. Ananthapadmanabhan, A. Lips, Langmuir 20 (2004) 5445–5453.
[36] K.D. Danov, P.A. Kralchevsky, Colloid J. 74 (2012) 172–185.
[37] T.D. Gurkov, P.A. Kralchevsky, K. Nagayama, Colloid Polym. Sci. 274 (1996) 227–238.
[38] O. Stern, Ztschr. Elektrochem. 30 (1924) 508–516.
[39] J.N. Israelachvili, Intermolecular and Surface Forces, Academic Press, London, 2011.
[40] K.D. Danov, P.A. Kralchevsky, K.P. Ananthapadmanabhan, A. Lips, J. Colloid Interface Sci. 300 (2006) 809–813.
[41] F.M. Menger, S.A.A. Rizvi, Langmuir 27 (2011) 13975–13977.
[42] P.X. Li, R.K. Thomas, J. Penfold, Langmuir 30 (2014) 6739–6747.
[43] V.V. Kalinin, C.J. Radke, Colloids Surf. A 114 (1996) 337–350.
[44] M.L. Corrin, W.D. Harkins, J. Am. Chem. Soc. 69 (1947) 683–688.
[45] S.S. Tzocheva, P.A. Kralchevsky, K.D. Danov, G.S. Georgieva, A.J. Post, K.P. Ananthapadmanabhan, J. Colloid Interface Sci. 369 (2012) 274–286.
[46] S.S. Tzocheva, K.D. Danov, P.A. Kralchevsky, G.S. Georgieva, A.J. Post, K.P. Ananthapadmanabhan, J. Colloid Interface Sci. 449 (2015) 46–61.
[47] D.J. Mitchell, B.W. Ninham, J. Phys. Chem. 87 (1983) 2996–2998.